Absolute single-ion thermometry

Vincent Tugayé, Jean-Pierre Likforman, Samuel Guibal, and Luca Guidoni*
Université Paris–Diderot, Sorbonne Paris Cité, Laboratoire Matériaux et Phénomènes Quantiques, UMR 7162 CNRS, F-75205 Paris, France

(Received 27 September 2018; published 11 February 2019)

We describe and experimentally implement a single-ion local thermometry technique with absolute sensitivity adaptable to all laser-cooled atomic ion species. The technique is based on the velocity-dependent spectral shape of a quasi-dark resonance tailored by two driving fields in a $J \rightarrow J$ transition such that the two fields can be derived from the same laser source, leading to a negligible relative phase shift. We validated the method and tested its performance in an experiment on a single $^{88}Sr^{+}$ ion cooled in a surface radio-frequency trap. We first applied the technique to characterize the heating rate of the surface trap. We then measured the stationary temperature of the ion as a function of cooling laser detuning in the Doppler regime. The results agree with theoretical calculations, with an absolute error smaller than 100 μK at 500 μK, in a temperature range between 0.5 and 3 mK and in the absence of adjustable parameters. This simple-to-implement and reliable method opens the way to fast absolute measurements of single-ion temperatures in future experiments dealing with heat transport in ion chains or thermodynamics at the single-ion level.

DOI: 10.1103/PhysRevA.99.023412

Laser-cooled trapped ions offer the opportunity for a precise quantum control at the single-particle level [1] that triggered the development of ion-based platforms dedicated to quantum information processing [2,3]. Cold-ion-based systems have also been proposed and applied for testing thermodynamics in the quantum regime [4,5] and quantum heat transport in network chains [6–9]. The latter application needs the development of thermometry techniques effective for characterizing in a short time the velocity distribution of a single-ion that possibly interacts with a rich environment. Since the first demonstrations of laser cooling of trapped ions [10,11], experimental thermometry tools have been developed together with theoretical models predicting stationary temperatures, for instance, in the case of Doppler cooling [12,13]. Among the thermometry techniques we can distinguish between three main families.

In a first approach the spatial distribution of a single ion in a trap is measured by acquiring a time-averaged image of its fluorescence. The knowledge of the stiffness of the trap and the measurement of the spot size allow for the retrieval of the ion energy distribution. This technique, introduced in early experiments [14], has been implemented to reach milli-Kelvin sensitivity [15,16] and to measure anomalous heating in a surface trap [17]. Spatial thermometry is only adapted to single-ion experiments and the limited knowledge of the point spread function of the imaging system affects both the accuracy and the precision of the method, which reaches its best performances in shallow traps.

A second family of thermometry techniques exploits the sensitivity to the ion motional state of the optically addressed narrow vibrational transitions in a trap (either quadrupole- or Raman-addressed). This technique has been introduced by Monroe and co-workers [18] and allows for the measurement of the average vibrational occupation number $\bar{n}$ in a given vibrational mode. Sideband spectroscopy has been used for the first studies of the heating rates associated with ion traps [19]; it addresses relatively low temperature ranges ($\bar{n} < 5$), but can be extended towards higher temperatures by measuring collapses and revivals of vibrational populations [20–22]. While extremely powerful, these techniques are only able to characterize normal modes of oscillation sequentially; this limitation may be a serious drawback for experiments that involve measurements of many vibrational modes.

The third approach to thermometry, which we address here, is based on the modifications of the photon scattering rate induced by the Doppler effect and has been used in the first demonstrations of laser cooling of ions [10,11]. More recently this approach has been exploited by recording and analyzing the transient photon scattering rate during the Doppler cooling of an ion (Doppler recooling technique [23,24]). This technique has been extended to ions with richer level structures (e.g., Ca^{+} and Sr^{+}), either using incoherent repumping schemes [25] or including the multilevel structure in the analysis of transient photon scattering [22,26]. The relatively large linewidth of the usual cooling transitions ($\simeq 2\pi \times 20$ MHz) implies that Doppler recooling thermometry can only address the measurement of relatively high temperatures ($T > 1$ K) with a millisecond characteristic time. However, multilevel ions addressed by at least two laser beams may also display the so-called "dark resonance" phenomenon [27,28] that may originate spectral features with narrow linewidths [29]. These dark resonances depend on the motional state and may indeed be used for cooling the ions below the Doppler limit [30–34], for evaluating the ion excess micromotion [35], and for thermometry purposes [36,37]. The main advantage of cooling and thermometry methods based on dark resonances is their ability to address (or sense) all vibrational modes without the need of multiplexing. In the case of thermometry this ability allows for a fast probing of the velocity distribution of a single

*luca.guidoni@univ-paris-diderot.fr

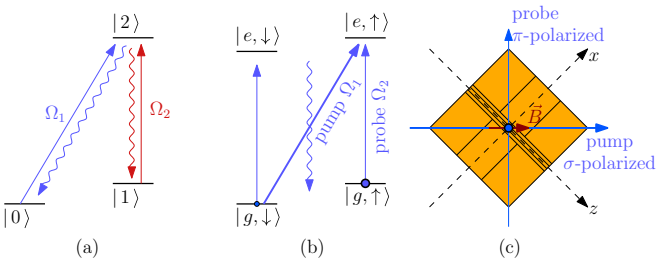

FIG. 1. (a) Energy level structure of a Λ system that allows for the presence of a dark state. (b) Quasi-Λ system considered in this paper. (c) Pump and probe beam geometry with respect to the trap axes.

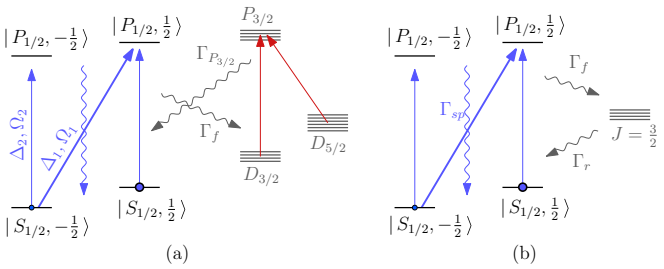

FIG. 2. Incoherent repumping scheme. (a) Considering the level structure of the $^{88}Sr^{+}$ ion, population trapping in the metastable level $D_{3/2}$ is avoided by exciting the $D_{3/2} \rightarrow P_{3/2}$ and $D_{5/2} \rightarrow P_{3/2}$ transitions. In this way no coherence is driven between the $S_{1/2}$ or $P_{1/2}$ levels and the other states. (b) Simplified level structure in which the $D_{3/2}$, $D_{5/2}$, and $P_{3/2}$ levels are replaced by a single $J = 3/2$ level that is incoherently populated with a rate Γ_f and decays into the $S_{1/2}$ level with an effective rate Γ_r.

ion that may be interacting with rich environments (Coulomb crystals or thermal baths) [37].

In this paper we present an implementation of dark-resonance thermometry and demonstrate its ability to measure absolute temperatures (accuracy and precision in the sub-mK range) in the absence of calibrations with other methods. This substantial improvement is obtained by addressing two transitions with two driving fields derived by the same laser source. This configuration eliminates phase stability issues that limited the precision in previous experiments [37]. The fit of the spectral experimental data with the solutions of the optical Bloch equations (OBEs), in the absence of *ad hoc* parameters, allowed us to obtain a measurement of absolute temperatures between 0.2 and 3 mK. We also calculated that the range of applicability is adjustable up to 200 mK. In order to test experimentally this thermometry tool we implemented it with a single Sr^{+} ion loaded and cooled in a surface trap. We exploited the measured temperatures to characterize the heating rate of the trap and to verify in an absolute way the theoretical law describing the stationary temperature reached with one-beam Doppler cooling [13]. We also demonstrated that this dark-resonance approach is capable of cooling the ion well in the sub-Doppler regime [down to $T_z = 0.13(1)$ mK] with a mechanism reminiscent of electromagnetically induced transparency (EIT) cooling [30] but in a different regime.

I. THEORY

Let us start considering a three-level atom in a Λ configuration driven by two laser fields with wave vectors $\vec{k}_1$ and $\vec{k}_2$ [see Fig. 1(a)]. For an atom at rest, a fluorescence spectrum obtained by scanning the detuning of one beam while keeping the other detuning constant displays a dark resonance: a sharp drop in the scattering rate. This feature is due to the presence of a "dark state":

$$|\psi_D\rangle(t) \propto \Omega_2|0\rangle - \Omega_1 e^{i\varphi(t)}|1\rangle, \tag{1}$$

where $\varphi(t) = (\Delta_2 - \Delta_1)t + \varphi_2(t) - \varphi_1(t)$ and Δ_i, Ω_i, and $\varphi_i(t)$ are the detunings, the Rabi frequencies, and the phases of the driving fields ($i = 1$ and 2) [38]. As long as φ does not depend on time, $|\psi_D\rangle$ is not coupled to the driving fields: for $\Delta_1 = \Delta_2$ and if $[\varphi_2(t) - \varphi_1(t)]$ is constant a dark resonance shows up because the electronic population is optically pumped in $|\psi_D\rangle$. For an atom that moves with velocity $\vec{v}$, the Doppler effect induces an additional detuning, $\delta_i = \vec{k}_i \cdot \vec{v}$ ($i = 1$ and 2), giving

$$\dot{\varphi}_{\text{Doppler}} = \delta_2 - \delta_1 = (\vec{k}_1 - \vec{k}_2) \cdot \vec{v}. \tag{2}$$

Atomic motion along the $\vec{k}_1 - \vec{k}_2$ direction breaks the dark-state condition and allows us to infer the velocity distribution from the contrast and shape of the dark resonance [36,37].

In a previous implementation of dark-resonance thermometry with $^{40}Ca^{+}$ ions, the frequency difference between the two driving lasers was very large (several hundreds of THz). In this situation it may be very challenging to stabilize the relative phase of the driving fields: the contrast and shape of the dark resonance are affected by this technical issue. Phase instability may be taken into account by an *ad hoc* parameter in the OBE but still sets the limit to the precision of the technique [37]. On the contrary, if the two lower levels of the Λ system lie in the ground-state manifold [36], the two driving fields can be derived by the same laser source and their relative phase drift becomes negligible. This is our approach: Here we consider a generalized dark resonance in a quasi-Λ system in which the two lower levels are Zeeman sublevels of the ground state of an ion. As shown in Fig. 1(b) a $J = 1/2 \rightarrow J' = 1/2$ transition is driven by a σ^{+}-polarized pump beam and a π-polarized probe beam with Rabi frequencies Ω_1 and Ω_2, respectively. The quantification axis is imposed by the magnetic field B. In this configuration, there is a residual coupling between the $|g,\downarrow\rangle$ state and the $|e,\downarrow\rangle$ state that shortens the lifetime of $|\psi_D\rangle$ and thus reduces the contrast of the dark resonance. However this is not a limiting factor because the choice of $\Omega_1 > \Omega_2$ allows us to create a state arbitrarily close to a dark state [reduced weight in the first term on the right-hand side of Eq. (1)].

To obtain the theoretical line shape of a fluorescence spectrum for an ion at rest in the configuration of Fig. 1(b), we solve the OBE in the stationary regime within the rotating-wave approximation [39].

In the following we consider the $^{88}Sr^{+}$ ion for the calculations but the method may be applied to other level structures. The low-lying energy-level structure of $^{88}Sr^{+}$ (including metastable states) is shown in Fig. 2(a). In order to avoid the trapping of electronic population in the metastable $D_{3/2}$ state and the presence of two-colors dark resonances involving $S_{1/2}$

and $P_{1/2}$ states we adopt an incoherent repumping scheme [25]. This can be obtained by addressing the $D_{3/2} \rightarrow P_{3/2}$ and $D_{5/2} \rightarrow P_{3/2}$ transitions with two laser beams.

We obtain the density matrix ρ of the internal states of the ion in the stationary regime by solving the OBE in the form:

$$\frac{d\rho}{dt} = \frac{i}{\hbar}[\mathcal{H}, \rho] + \mathcal{L}[\rho] = 0. \tag{3}$$

We found that the solution of the complete OBE can be very well approximated by the solution of a simplified system in which the $D_{3/2}$, $D_{5/2}$, and $P_{3/2}$ levels are replaced by a single $J = 3/2$ level that is incoherently populated with a rate Γ_f and decays into the $S_{1/2}$ level with an effective rate Γ_r [see Fig. 2(b)]:

$$\Gamma_r = \frac{\rho_{P_{3/2}}}{\rho_{P_{3/2}} + \rho_{D_{3/2}} + \rho_{D_{5/2}}} \Gamma_{P_{3/2}}. \tag{4}$$

In order to speed up the numerical calculations we used this approximation that also has the advantage of describing the repumping process in terms of the single parameter Γ_r. This parameter can be determined by performing a one-beam Doppler cooling experiment in which we estimate the ion scattering rate at saturation on the $P_{1/2} \rightarrow S_{1/2}$ transition as

$$\rho_{P_{1/2},\mathrm{sat}} = \frac{1}{2 + \frac{\Gamma_f}{\Gamma_r}}. \tag{5}$$

To write the Hamiltonian $\mathcal{H}$ of the system we set the origin of energies to the $|P_{1/2}, \frac{1}{2}\rangle$ level with a null magnetic field. By adopting the rotating-wave approximation, in the $|S_{1/2}, -\frac{1}{2}\rangle$, $|S_{1/2}, \frac{1}{2}\rangle$, $|P_{1/2}, -\frac{1}{2}\rangle$, $|P_{1/2}, \frac{1}{2}\rangle$ basis, the Hamiltonian then reads as follows:

$$\mathcal{H} = \hbar \begin{bmatrix} -B + \Delta_2 & 0 & \sqrt{\frac{1}{3}}\frac{\Omega_2^*}{2} & 0 \\ 0 & B + \Delta_1 & \sqrt{\frac{2}{3}}\frac{\Omega_1^*}{2} & -\sqrt{\frac{1}{3}}\frac{\Omega_2^*}{2} \\ \sqrt{\frac{1}{3}}\frac{\Omega_2}{2} & \sqrt{\frac{2}{3}}\frac{\Omega_1}{2} & -\frac{B}{3} & 0 \\ 0 & -\sqrt{\frac{1}{3}}\frac{\Omega_2}{2} & 0 & \frac{B}{3} + \Delta_1 - \Delta_2 \end{bmatrix}, \tag{6}$$

where the Zeeman energy splitting is given in units of frequency: $B = \frac{\mu_B}{\hbar}|\vec{B}|$. The Hamiltonian also depends on the detunings and Rabi frequencies of the pump and probe beams Δ_1, Ω_1 and Δ_2, Ω_2, respectively.

Spontaneous decay is taken into account by the Linblad operator $\mathcal{L}$ [39]:

$$\mathcal{L}[\rho] = \sum_{f,i} -\frac{1}{2}(C_{fi}^\dagger C_{fi}\rho + \rho C_{fi}^\dagger C_{fi}) + C_{fi}\rho C_{fi}^\dagger, \tag{7}$$

$$C_{fi} = \sqrt{\Gamma_{fi}}|f\rangle\langle i|, \tag{8}$$

where the subscripts i and f represent the initial level and the final level of the specific spontaneous decay channel. The decay rate matrix Γ in the $|S_{1/2}, -\frac{1}{2}\rangle$, $|S_{1/2}, \frac{1}{2}\rangle$, $|P_{1/2}, -\frac{1}{2}\rangle$, $|P_{1/2}, \frac{1}{2}\rangle$, $|\frac{3}{2}, -\frac{3}{2}\rangle$, $|\frac{3}{2}, -\frac{1}{2}\rangle$, $|\frac{3}{2}, \frac{1}{2}\rangle$, $|\frac{3}{2}, \frac{3}{2}\rangle$ basis reads as follows:

$$\Gamma = \begin{bmatrix} 0 & 0 & \frac{1}{3}\Gamma_{sp} & \frac{2}{3}\Gamma_{sp} & \Gamma_r & \frac{2}{3}\Gamma_r & \frac{1}{3}\Gamma_r & 0 \\ 0 & 0 & \frac{2}{3}\Gamma_{sp} & \frac{1}{3}\Gamma_{sp} & 0 & \frac{1}{3}\Gamma_r & \frac{2}{3}\Gamma_r & \Gamma_r \\ 0 & 0 & 0 & 0 & 0 & 0 & 0 & 0 \\ 0 & 0 & 0 & 0 & 0 & 0 & 0 & 0 \\ 0 & 0 & \frac{1}{2}\Gamma_f & 0 & 0 & 0 & 0 & 0 \\ 0 & 0 & \frac{1}{3}\Gamma_f & \frac{1}{6}\Gamma_f & 0 & 0 & 0 & 0 \\ 0 & 0 & \frac{1}{6}\Gamma_f & \frac{1}{3}\Gamma_f & 0 & 0 & 0 & 0 \\ 0 & 0 & 0 & \frac{1}{2}\Gamma_f & 0 & 0 & 0 & 0 \end{bmatrix}, \tag{9}$$

where Γ_{sp} is the decay rate on the $P_{1/2} \rightarrow S_{1/2}$ transition and Γ_f is the decay rate on the $P_{1/2} \rightarrow D_{3/2}$ transition.

The scattering rate S is given by $S = \Gamma_e \rho_{ee}$, where Γ_e is the inverse of the lifetime of the excited state and ρ_{ee} is the sum of the populations in the excited-state sublevels. As shown in Fig. 3 (solid thick line), a dark resonance occurs in the fluorescence spectrum for $\Delta_2 = \Delta_2^d$ (two-photon resonance condition); the precise value of Δ_2^d depends mainly on the pump detuning Δ_1 and on the Zeeman shifts. We consider then an ion moving in a harmonic potential and, to simplify numerical calculations, we assume that the internal-state evolution is much faster than the ion secular oscillation (weak binding approximation). We describe classically the motional degrees of freedom and we consider a Maxwell-Boltzmann thermal velocity distribution described by the temperature T_z such that $\hbar\omega_z \ll k_B T_z$, where ω_z is the secular frequency along the z axis [Fig. 1(c)]. We also neglect the micromotion in the z direction (ideal linear trap). We then calculate the scattering rate for a moving ion as a two-dimensional convolution of steady-state solutions for an ion at rest with the distribution of velocity-dependent detunings δ_1 and δ_2. Calculations show that, as expected, the motion along $\vec{k}_1 + \vec{k}_2$ (x direction) does not affect significantly the shape of the fluorescence spectrum.

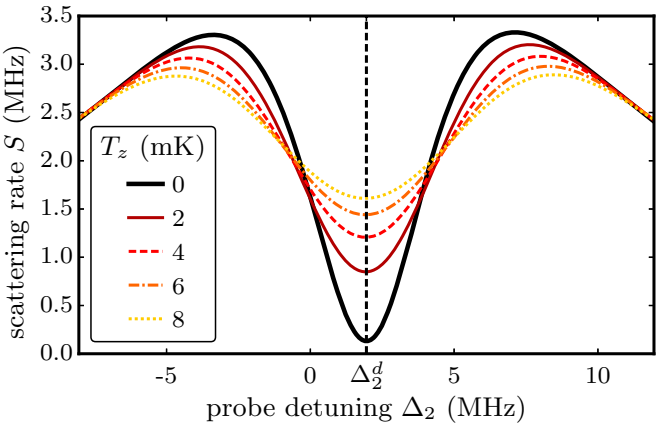

FIG. 3. Calculated fluorescence spectra in the presence of a thermal velocity distribution for a motion along the z axis and for several temperatures T_z. The ion parameters correspond to the $5s\,^2S_{1/2} \rightarrow 5p\,^2P_{1/2}$ transition of $^{88}Sr^+$. The other parameters for the calculation are $\Omega_1 = 12$ MHz, $\Omega_2 = 4$ MHz, $\Delta_1 = -3.7$ MHz, and $B = 2 \times 10^{-4}$ T.

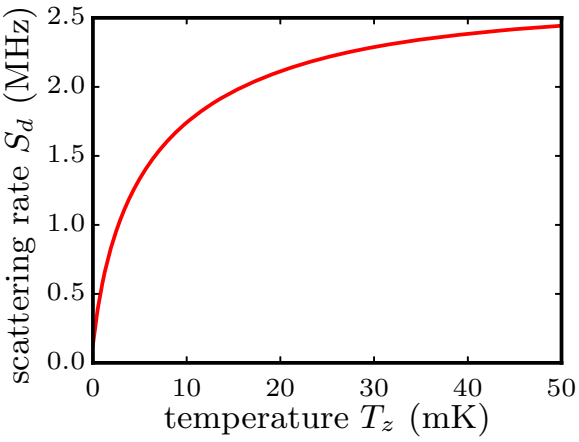

FIG. 4. Calculated scattering rate $S_d(T_z)$ at the center of the dark resonance as a function of the temperature. The parameters used for the calculation are $\Omega_1 = 12$ MHz, $\Omega_2 = 4$ MHz, $\Delta_1 = -3.7$ MHz, $\Delta_2 = 2$ MHz, and $B = 2 \times 10^{-4}$ T.

On the contrary, thermal motion along the $\vec{k}_1 - \vec{k}_2$ direction (z axis) affects both the contrast and the width of the dark resonance, as can be seen in Fig. 3. The parameters injected in this calculation correspond to the $5s\,^2S_{1/2} \rightarrow 5p\,^2P_{1/2}$ transition of the $^{88}Sr^+$ ion; the beam parameters are set to $\Omega_1 = 12$ MHz, $\Omega_2 = 4$ MHz, and $\Delta_1 = -3.7$ MHz; the magnetic field is $B = 2 \times 10^{-4}$ T. In particular it is possible to calculate with the same set of parameters the scattering rate $S_d = S(\Delta_2 = \Delta_2^d)$ as a function of the temperature T_z. As shown in Fig. 4, S_d is a monotonous function of T_z. Therefore, the knowledge of the parameters Ω_1, Ω_2, B, Δ_1, and $\Delta_2 = \Delta_2^d$ allows us to calculate the inverse function $T_z(S_d)$. In order to access different temperature ranges it is possible to tailor the width of the dark resonance by changing the pump and probe Rabi frequencies, while keeping constant their ratio (that fixes the contrast at zero temperature).

In the following we describe a numerical analysis that allows us to relate the linewidth of the dark resonance, the scattering rate, and the acquisition time necessary to reach a target statistical signal-to-noise ratio (SNR) affecting the temperature measurement. In the thermometry experiments we measure on a photon counter the experimental scattering rate $S_{\rm exp}$ of the photons scattered by the ion addressed by the pump and probe beams. The intrinsic scattering rate S is obtained taking into account the collection efficiency of the setup η (measured independently [40]) as $S_{\rm exp} = \eta \times S$. We consider an accumulation time $\tau_{\rm acc}$ during which we detect N photons. Assuming a Poissonian distribution for N, the mean number of photon counts $\langle N \rangle$ and its variance $(\Delta N)^2 = \langle N^2 \rangle - \langle N \rangle^2$ are given by

$$\langle N \rangle = (\Delta N)^2 = \eta S \tau_{\rm acc}. \tag{10}$$

For a given set of experimental parameters Δ_1, Ω_1, Δ_2, and Ω_2, the temperature of the ion is a function $T_z(S_d)$ of the scattering rate S_d measured at the center of the dark resonance. Up to the first order of the function $T_z(S_d)$ we can write the standard variation ΔT_z affecting the temperature as

$$\Delta T_z = \frac{dT_z}{dS_d}\Delta S_d = \frac{dT_z}{dS_d}\sqrt{\frac{S_d}{\eta \tau_{\rm acc}}}. \tag{11}$$

In terms of the function $S_d(T_z)$ (Fig. 4) we then have

$$\frac{\Delta T_z}{T_z} = \frac{1}{\sqrt{\eta \tau_{\rm acc}}}\frac{\sqrt{S_d(T_z)}}{T_z S_d'(T_z)}. \tag{12}$$

The numerical calculation of the fractional uncertainty (12) allows us to optimize the experimental parameters in order to measure a given temperature T_z. We found, for example, that a good match between the dark resonance and the thermal Doppler linewidths maximizes the signal-to-noise ratio on T_z. We have also studied the applicability range of the method by imposing (somewhat arbitrarily) a maximum accumulated probing time of $\tau_{\rm acc} = 20$ s and a target fractional uncertainty of $\Delta T_z/T_z = 1/10$. We obtain an accessible temperature range between 2×10^{-2} and 2×10^2 mK for an experimental parameter set well accessible with standard laser sources. Let us now discuss the origin of systematic errors affecting T_z. The dominant systematic errors affecting the retrieved temperature have their origin in the imperfect "one shot" estimation of the parameters Ω_1, Ω_2, and B that describe the line shape of the dark resonance, necessary to parametrize the function $S_d(T_z)$. The statistical error affecting this imperfect estimation can be retrieved from the fitting procedure; nevertheless all the temperatures measured with the same set of parameters display correlated (systematic) errors.

II. EXPERIMENTS

The experiments are realized using single $^{88}Sr^+$ ions trapped in a symmetric five-wire surface trap [41].The details concerning the trap design and the experimental setup can be found in Ref. [42].

In brief, we drive the trap with a radio-frequency (rf) voltage oscillating at $2\pi \times 8.9$ MHz and static (dc) voltages leading to secular frequencies $\omega_z/2\pi = 98$ kHz, $\omega_x/2\pi = 510$ kHz, and $\omega_y/2\pi = 370$ kHz. We used a time-correlated single-photon counting technique [43] in order to minimize excess micromotion. Along the x direction we estimate a residual amplitude of $x_0 < 4$ nm (equivalent pseudotemperature $T_x^\mu < 240$ μK). According to the trap field calculations [44], a small rf field component along z exists, leading to a possible excess z micromotion. We estimate that, after compensation, its residual amplitude is $z_0 < 1$ nm (equivalent pseudotemperature $T_z^\mu < 25$ μK). Let us mention that the equivalent pseudotemperature originated by intrinsic (i.e., not excess) micromotion is negligible in the z direction (some thousandth of the secular temperature), while, as expected, it is a conspicuous fraction ($\simeq$80%) of secular temperature in the x direction.

We address the $5s\,^2S_{1/2} \rightarrow 5p\,^2P_{1/2}$ transition; to avoid optical pumping in the $4d\,^2D_{3/2}$ we repump the electronic populations with an incoherent scheme [25] that addresses simultaneously the $4d\,^2D_{3/2} \rightarrow 5p\,^2P_{3/2}$ and $4d\,^2D_{5/2} \rightarrow 5p\,^2P_{3/2}$ transitions. The fluorescence spectra are acquired using a sequential approach to neglect the mechanical effect of the beams during the probing phase [45,46]. We used probing

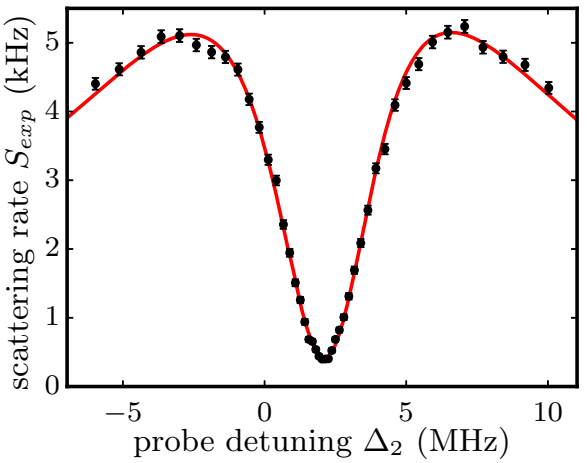

FIG. 5. Averaged experimental fluorescence spectrum (black dots). The pump detuning is $\Delta_1 = -3.7$ MHz and the ion is precooled to a sub-Doppler temperature with a cooling phase in which the probe is tuned to $\Delta_2 = 1.7$ MHz. The free parameters obtained from the numerical fit (red line) are $\Omega_2 = 3.78(1)$ MHz, $\Omega_1 = 10.7(1)$ MHz, $B = 2.06(1) \times 10^{-4}$ T, and ion temperature $T = 0.128(7)$ mK. The uncertainties do not take into account systematic shifts.

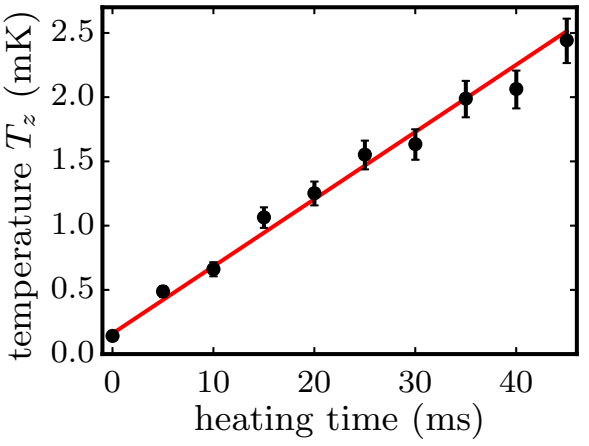

FIG. 6. Averaged retrieved temperature T_z as a function of the heating time (black dots). The heating rate of the trap (slope of the fit, red line) is 52(1) mK/s. Error bars are ± 1 standard deviation (both statistical and systematic).

phase durations in the range 10–100 μs such that the number of spontaneous photons emitted during temperature measurements was less than 25. As the recoil temperature for $^{88}Sr^+$ is $\frac{\hbar^2 k^2}{m_{Sr} k_B} = 1.22$ μK, we expect a recoil heating in the tens of micro-Kelvin range. We measure on a photon counter the scattering rate $S_{\text{exp}} = S \times \eta$, where $\eta = 1.95(5) \times 10^{-3}$ is the collection efficiency of the setup and S is the intrinsic scattering rate. The detunings Δ_1 and Δ_2 are imposed by two acousto-optic modulators that shift with a negligible phase noise a common laser beam (that is frequency locked to an atomic reference with a precision better than 100 kHz). As a first check we acquired several fluorescence spectra for different Ω_1, Ω_2, and B for an ion cooled close to the Doppler limit. Numerical fits with the solution of the OBE are in excellent agreement with the experimental spectra and the parameters extracted from the fits follow the variations imposed on the experimental parameters and give a constant temperature T_z consistent with the Doppler limit. Let us mention that, as this is a single-ion experiment, the temperature T_z may only be retrieved by averaging over many realizations the velocity-dependent scattering rate S_{exp}. The sequential acquisition that consists of repeated preparation and probing phases allows us to obtain such an averaging. For a fixed set of known parameters Ω_1, Ω_2, B, Δ_1, and $\Delta_2 = \Delta_2^d$, T_z can be retrieved from a measurement of the average scattering rate S_d (see above). In the following we adopt this approach, faster than the acquisition of a full fluorescence spectrum for each temperature. In order to precisely evaluate the Ω_1, Ω_2, and B parameters we acquire and fit a preliminary calibration spectrum, such as the one presented in Fig. 5. In this specific case the pump detuning is $\Delta_1 = -3.7$ MHz and the ion is precooled to a sub-Doppler temperature with a cooling phase in which the probe is tuned to $\Delta_2 = 1.7$ MHz. The free parameters obtained from the numerical fit (red line) are $\Omega_2 = 3.78(1)$ MHz, $\Omega_1 = 10.7(1)$ MHz, $B = 2.06(1) \times 10^{-4}$ T, and ion temperature $T = 0.128(7)$ mK.

As a first application we have measured the heating rate of the surface trap affecting the motion along the z axis. For that purpose we prepared the ion at an initial temperature T_{in} and then measured its temperature after a heating phase during which laser cooling is switched off. The results of these measurements are shown in Fig. 6 and display the expected linear behavior that allow us to measure a heating rate of 52(1) mK/s. In order to extend the range of these measurements we precooled the ion to a sub-Doppler temperature of $T_{\text{in}} = 0.20(5)$ mK (with our geometry the one-beam Doppler limit for Sr^+ is $T_D = 0.47$ mK), taking advantage of the mechanism reminiscent of the EIT cooling that operates with Δ_2 tuned on the low-frequency side of the dark resonance. This cooling method occurs in a completely different regime with respect to previous realizations of EIT cooling [30]; the complete description of the mechanisms involved is beyond the scope of this paper. To validate the absolute character of this thermometry technique we have measured the ion temperature as a function of the detuning of a Doppler cooling beam at low intensity [16]. Indeed in this regime it is possible to calculate analytical expressions describing both the cooling dynamics and the stationary temperature [13]. The experimental sequence includes two cooling phases. The first step has a duration of 20 ms and is performed at optimal detuning, allowing us to reach a temperature on the order of 0.5 mK with a theoretical characteristic time of 320 μs. The second cooling step, performed at intensity $I \ll I_{\text{sat}}$ (where I_{sat} is the saturation intensity), has a duration set to ten times the characteristic cooling time as calculated from the theory. The measured temperature of the ion as a function of the cooling beam detuning is shown in Fig. 7 (black dots). In order to compare this result with the theoretical prediction, we acquire an experimental fluorescence spectrum (scattering rate as a function of cooling beam detuning) at the same (low) cooling beam intensity. The sequential character of the acquisition and the incoherent repumping scheme allows us to describe the spectrum in terms of a pure Lorentzian line shape.

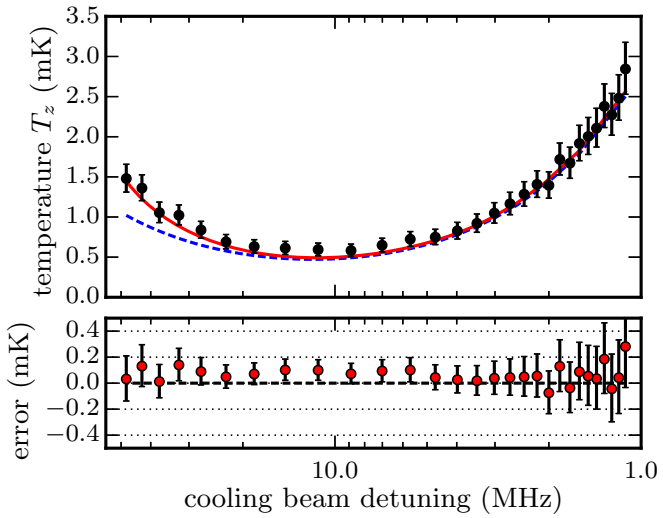

FIG. 7. Averaged retrieved temperature T_z as a function of the Doppler-cooling beam detuning (black dots). Measurements are obtained in the low-intensity regime $I \ll I_{\text{sat}}$. The solid red line (blue dashed line) is the result of a calculation of the stationary temperature including (not including) the trap heating rate (see Fig. 6). The bottom panel of the figure shows the residuals (red dots) with the associated statistical standard deviation.

We then inject the two parameters describing the Lorentzian scattering rate in the theoretical model of Doppler cooling and obtain the stationary temperature as a function of cooling beam detuning (dashed line in Fig. 7), in the absence of adjustable parameters. The discrepancy with the experimental data observed at large detunings is dominated by the effect of the trap heating rate (see above), as shown by the stationary temperature obtained with calculations that include this term (solid line in Fig. 7). The error bars in Fig. 7 (± 1 standard deviation) are calculated taking into account both photon count statistics and calibration uncertainties.

III. CONCLUSION

In conclusion we demonstrated a thermometry technique that we implemented with a single Sr^+ ion loaded and cooled in a surface trap. We applied the technique to characterize the heating rate of the trap and to verify, in an absolute way, the theoretical law describing the stationary temperature reached with one-beam Doppler cooling. The excellent agreement between the calculations and the experimental measurements over a large range of detunings demonstrates the reliability of the method and opens the way to fast (the probing time in a sequence is on the order of 10 μs) and directional single-ion absolute thermometry.

Extensions of this work may apply to cases in which nonthermal distributions are expected, as long as we are able to inject the shape and the characteristics of a parametrized velocity distribution in the model (i.e., hypothesis about the shape of the velocity distribution). As an example, by inverting the propagation direction of one beam it would be possible to probe the velocity distribution along the x direction that will contain contributions both from the thermal secular motion and from the intrinsic (nonthermal) micromotion, with similar weight. Let us mention that, if a non-negligible rf field is present, depending on its frequency an analysis beyond the stationary regime (i.e., involving the numerical solution of the time-dependent OBE) will be necessary, without affecting the principles of the technique but beyond the scope of this paper. Nonthermal distributions obtained with sub-Doppler laser cooling should also be measurable with this method, provided that the number of photons scattered during the probing phase induces a recoil heating negligible with respect to the initial temperature. In the particular case of surface traps, information about the velocity distribution along the y direction is not accessible. However in three-dimensional traps this limitation could be easily lifted, allowing for the orientation of the $\vec{k}_1 - \vec{k}_2$ vector such that a projection exists along all the motional modes of the trap. In the case of nontrivial environments (e.g., thermodynamics of an ion in a linear chain or an ion in contact with atoms) the technique may be applied if spatially resolved single-ion addressing is implemented, at least with one of the two probing beams. The absolute character of the method will probably open interesting perspectives in these fields.

ACKNOWLEDGMENTS

We thank M. Apfel, P. Lepert, and M. Nicolas for technical support. This study was partly funded by Région Ile-de-France through the DIM Nano-k (DEQULOT grant).

[1] D. J. Wineland, Rev. Mod. Phys. **85**, 1103 (2013).
[2] R. Blatt and D. Wineland, Nature (London) **453**, 1008 (2008).
[3] C. Monroe, R. Raussendorf, A. Ruthven, K. R. Brown, P. Maunz, L.-M. Duan, and J. Kim, Phys. Rev. A **89**, 022317 (2014).
[4] J. Roßnagel, O. Abah, F. Schmidt-Kaler, K. Singer, and E. Lutz, Phys. Rev. Lett. **112**, 030602 (2014).
[5] J. Roßnagel, S. T. Dawkins, K. N. Tolazzi, O. Abah, E. Lutz, F. Schmidt-Kaler, and K. Singer, Science **352**, 325 (2016).
[6] G.-D. Lin and L.-M. Duan, New J. Phys. **13**, 075015 (2011).
[7] A. Bermudez, M. Bruderer, and M. B. Plenio, Phys. Rev. Lett. **111**, 040601 (2013).
[8] N. Freitas, E. A. Martinez, and J. P. Paz, Phys. Scr. **91**, 013007 (2016).
[9] M. Ramm, T. Pruttivarasin, and H. Häffner, New J. Phys. **16**, 063062 (2014).
[10] W. Neuhauser, M. Hohenstatt, P. Toschek, and H. Dehmelt, Phys. Rev. Lett. **41**, 233 (1978).
[11] D. J. Wineland, R. E. Drullinger, and F. L. Walls, Phys. Rev. Lett. **40**, 1639 (1978).
[12] D. J. Wineland and W. M. Itano, Phys. Rev. A **20**, 1521 (1979).
[13] D. J. Wineland, W. M. Itano, J. C. Bergquist, and R. G. Hulet, Phys. Rev. A **36**, 2220 (1987).

[14] W. Neuhauser, M. Hohenstatt, P. E. Toschek, and H. Dehmelt, Phys. Rev. A **22**, 1137 (1980).
[15] B. G. Norton, E. W. Streed, M. J. Petrasiunas, A. Jechow, and D. Kielpinski, New J. Phys. **13**, 113022 (2011).
[16] S. Knünz, M. Herrmann, V. Batteiger, G. Saathoff, T. W. Hänsch, and T. Udem, Phys. Rev. A **85**, 023427 (2012).
[17] I. A. Boldin, A. Kraft, and C. Wunderlich, Phys. Rev. Lett. **120**, 023201 (2018).
[18] C. Monroe, D. M. Meekhof, B. E. King, S. R. Jefferts, W. M. Itano, D. J. Wineland, and P. Gould, Phys. Rev. Lett. **75**, 4011 (1995).
[19] Q. A. Turchette, D. Kielpinski, B. E. King, D. Leibfried, D. M. Meekhof, C. J. Myatt, M. A. Rowe, C. A. Sackett, C. S. Wood, W. M. Itano *et al.*, Phys. Rev. A **61**, 063418 (2000).
[20] D. M. Meekhof, C. Monroe, B. E. King, W. M. Itano, and D. J. Wineland, Phys. Rev. Lett. **76**, 1796 (1996).
[21] K. G. Johnson, B. Neyenhuis, J. Mizrahi, J. D. Wong-Campos, and C. Monroe, Phys. Rev. Lett. **115**, 213001 (2015).
[22] T. Sikorsky, Z. Meir, N. Akerman, R. Ben-shlomi, and R. Ozeri, Phys. Rev. A **96**, 012519 (2017).
[23] R. J. Epstein, S. Seidelin, D. Leibfried, J. H. Wesenberg, J. J. Bollinger, J. M. Amini, R. B. Blakestad, J. Britton, J. P. Home, W. M. Itano *et al.*, Phys. Rev. A **76**, 033411 (2007).
[24] J. H. Wesenberg, R. J. Epstein, D. Leibfried, R. B. Blakestad, J. Britton, J. P. Home, W. M. Itano, J. D. Jost, E. Knill, C. Langer *et al.*, Phys. Rev. A **76**, 053416 (2007).
[25] D. T. C. Allcock, J. A. Sherman, D. N. Stacey, A. H. Burrell, M. J. Curtis, G. Imreh, N. M. Linke, D. J. Szwer, S. C. Webster, A. M. Steane *et al.*, New J. Phys. **12**, 053026 (2010).
[26] Z. Meir, T. Sikorsky, N. Akerman, R. Ben-shlomi, M. Pinkas, and R. Ozeri, Phys. Rev. A **96**, 020701 (2017).
[27] G. Alzetta, A. Gozzini, L. Moi, and G. Orriols, Il Nuovo Cimento B (1971–1996) **36**, 5 (1976).
[28] E. Arimondo and G. Orriols, Lett. Nuovo Cimento (1971–1985) **17**, 333 (1976).
[29] I. Siemers, M. Schubert, R. Blatt, W. Neuhauser, and P. E. Toschek, Europhys. Lett. **18**, 139 (1992).
[30] G. Morigi, J. Eschner, and C. H. Keitel, Phys. Rev. Lett. **85**, 4458 (2000).
[31] C. F. Roos, D. Leibfried, A. Mundt, F. Schmidt-Kaler, J. Eschner, and R. Blatt, Phys. Rev. Lett. **85**, 5547 (2000).
[32] Y. Lin, J. P. Gaebler, T. R. Tan, R. Bowler, J. D. Jost, D. Leibfried, and D. J. Wineland, Phys. Rev. Lett. **110**, 153002 (2013).
[33] R. Lechner, C. Maier, C. Hempel, P. Jurcevic, B. P. Lanyon, T. Monz, M. Brownnutt, R. Blatt, and C. F. Roos, Phys. Rev. A **93**, 053401 (2016).
[34] D. T. C. Allcock, T. P. Harty, M. A. Sepiol, H. A. Janacek, C. J. Ballance, A. M. Steane, D. M. Lucas, and D. N. Stacey, New J. Phys. **18**, 023043 (2016).
[35] C. Lisowski, M. Knoop, C. Champenois, G. Hagel, M. Vedel, and F. Vedel, Appl. Phys. B **81**, 5 (2005).
[36] T. Peters, B. Wittrock, F. Blatt, T. Halfmann, and L. P. Yatsenko, Phys. Rev. A **85**, 063416 (2012).
[37] J. Rossnagel, K. N. Tolazzi, F. Schmidt-Kaler, and K. Singer, New J. Phys. **17**, 045004 (2015).
[38] E. Arimondo, V Coherent population trapping in laser spectroscopy, in *Progress in Optics*, edited by E. Wolf (Elsevier, Amsterdam, 1996), Vol. 35, pp. 257–354.
[39] C. Cohen-Tannoudji and D. Guery-Odelin, *Advances in Atomic Physics: An Overview* (World Scientific, Singapore, 2011).
[40] J.-P. Likforman, V. Tugayé, S. Guibal, and L. Guidoni, Phys. Rev. A **93**, 052507 (2016).
[41] J. Chiaverini, R. B. Blakestad, J. Britton, J. D. Jost, C. Langer, D. Leibfried, R. Ozeri, and D. J. Wineland, Quantum Inf. Comput. **5**, 419 (2005).
[42] B. Szymanski, R. Dubessy, B. Dubost, S. Guibal, J.-P. Likforman, and L. Guidoni, Appl. Phys. Lett. **100**, 171110 (2012).
[43] D. J. Berkeland, J. D. Miller, J. C. Bergquist, W. M. Itano, and D. J. Wineland, J. Appl. Phys. **83**, 5025 (1998).
[44] M. G. House, Phys. Rev. A **78**, 033402 (2008).
[45] A. Gardner, K. Sheridan, W. Groom, N. Seymour-Smith, and M. Keller, Appl. Phys. B **117**, 755 (2014).
[46] Z. Meir, O. Schwartz, E. Shahmoon, D. Oron, and R. Ozeri, Phys. Rev. Lett. **113**, 193002 (2014).